Biochemical and Biophysical Research Communications 533 (2020) 893–898

Contents lists available at ScienceDirect

Biochemical and Biophysical Research Communications

journal homepage: www.elsevier.com/locate/ybbrc

Synthesis of 13*R*,20-dihydroxy-docosahexaenoic acid by site-directed mutagenesis of lipoxygenase derived from *Oscillatoria nigro-viridis* PCC 7112

Jong-Jae Yi [a, b], Sun-Yeon Heo [a], Jung-Hyun Ju [a], Baek-Rock Oh [a], Woo Sung Son [b, **], Jeong-Woo Seo [a, *]

[a] *Microbial Biotechnology Research Center, Korea Research Institute of Bioscience and Biotechnology (KRIBB), Jeongeup-Si, 56212, Republic of Korea*
[b] *Department of Pharmacy, College of Pharmacy and Institute of Pharmaceutical Sciences, CHA University, Pocheon-Si, Gyeonggi-do, 11160, Republic of Korea*

ARTICLE INFO

Article history:
Received 7 September 2020
Accepted 20 September 2020
Available online 29 September 2020

Keywords:
Lipoxygenase
Coffa-brash principle
Site-directed mutagenesis
13*R*-HDHA
13*R*,20-diHDHA

ABSTRACT

Lipoxygenases (LOXs) are implicated in the biosynthesis of pro- and anti-inflammatory lipid mediators involved in immune cell signaling, most of which catalyze peroxidation of polyunsaturated fatty acids by distinct regio- and stereoselectivity. Current reports suggested that conserved amino acid, Gly in *R*-LOXs and Ala in *S*-LOXs, in the catalytic domain play an important role in determining the position as well as the stereochemistry of the functional group. Recently, we have confirmed that the catalytic specificity of cyanobacterial lipoxygenase, named Osc-LOX, with alanine at 296 was 13*S*-type toward linoleic acid, and producing a 17*S*- hydroxy-docosahexaenoic acid from docosahexaenoic acid (DHA). Here, we aimed to change the catalytic property of LOX from13*S*-LOX to 9*R*-LOX by replacing Ala with Gly and to produce a lipid mediators different from the wild-type using DHA. Finally, we succeeded in generating human endogenous a 13*R*-hydroxy-docosahexaenoic acid and a 13*R*,20-dihydroxy-docosahexaenoic acid from DHA through an enzymatic reaction using the Osc-LOX-A296G. Our study could enable physiological studies and pharmaceutical research for the 13*R*,20-dihydroxy-docosahexaenoic acid.

1. Introduction

Lipoxygenases (LOXs) are essential enzymes for biosynthesis of lipid mediators that are bioactive molecules involved in immune cell signaling. LOXs catalyze regio- and stereospecific peroxidation by the initiation of hydrogen abstraction in polyunsaturated fatty acids (PUFAs) containing one or more 1-*cis*,4-*cis*-pentadiene structure to yield hydroperoxides [1]. Hydrogen abstraction arises at a bis-allylic methylene group of PUFAs, and the peroxidation occurs either at the [+2] or [−2] carbon position by radical rearrangement [2]. linoleic acid (LA) containing one methylene group (C-11) can be peroxygenated at only two carbon positions (C-9 and/or C-13), whereas, docosahexaenoic acid (DHA) containing five methylene groups (C-6, C-9, C-12, C-15, and C-18) can be peroxygenated at ten positions (C-4, C-7, C-8, C-10, C-11, C-13, C-14, C-16, C17, and/or C-20), theoretically.

It has been known that the regio- and stereospecificity toward substrates of LOXs are controlled by three different hypothetical mechanisms as follows: (i) The orientation theory proposed that positional specificity is determined by the orientation, such as head-to-tail or tail-to-head, of substrates to entry into the catalytic pocket [3]. For instance, the difference in regiospecificty between 5*S*-LOX and 15*S*-LOX is due to the entry direction of the substrates. In the case of 5-LOX, the substrates enter into the substrate-binding pocket with its carboxylate group ahead. In contrast, for 15-LOX, the substrates slide into the catalytic site with its methyl-end first. (ii) The space theory suggested that regiospecificity depends on the volume of the catalytic pocket [4]. The volume of the active site of human 12-LOX is about 6% bigger than that of human 15-LOX resulting in a frameshift of the substrate is occurred. Thus, the position of peroxidation is determined by how deeply the substrate enters the active site. (iii) According to Coffa-Brash principle, Gly and Ala are key amino acids to determine of regio- and stereospecific (*R*/*S*) oxidation at C-1 and C-5 of the1-*cis*,4-*cis*-pentadiene.

* Corresponding author.
** Corresponding author.
E-mail address: jwseo@kribb.re.kr (J.-W. Seo).

https://doi.org/10.1016/j.bbrc.2020.09.079
0006-291X/

Ala is highly conserved in *S*-type LOXs, whereas relatively the smaller amino acid Gly is conserved in *R*-type LOXs [5]. If these three mechanisms could be applied to LOXs, they could be used as tools to produce the lipid mediators that exist in the human immune system but cannot be generated via *in vitro* enzyme reaction.

In our previous study, it has been identified that cyanobacterial lipoxygenase (Osc-LOX) derived from *Oscillatoria nigro-viridis* PCC 7112 has alanine at 296 position and the catalytic specificity was 13*S*-type toward LA. Also, it has been confirmed that wild-type Osc-LOX generates a 17*S*-hydroperoxy-DHA as intermediate product from DHA by hydrogen abstraction for the C-15 methylene group (under revision). The aim of this study was to investigate the applicability of the Coffa-Brash principle for Osc-LOX and to observe the changes in the regio- and stereospecificity of the enzyme. Hence, we carried out site-directed mutagenesis to substitute 296 alanine with glycine.

2. Materials and methods

2.1. Mutagenesis and expression of osc-LOX-A296G

The DNA sequence of wild-type *osc-lox* (accession number AFZ09286.1, 1713 bp) was found in the GeneBank database. Site-directed mutagenesis of Osc-LOX derived from *Oscillatoria nigro-viridis* PCC 7112 was designed by multiple sequence alignment analysis with conserved sequence of heterologous. The gene encoding Osc-LOX-A296G was synthesized by Bioneer Inc. and it was inserted between *Nde*I and *Xho*I (New England Biolabs, Beverly, MA, USA) sites of the pET-28a plasmid (Novagen, Madison, WI, USA) with the N-terminal His-tag. *E. coli* DH5α (RBC, Banqiao, Taiwan) was used to amplify of plasmids number. *E. coli* BL21 (DE3) (Novagen, Madison, WI, USA) was transformed with constructed plasmids and used for enzyme expression. Host cells harboring pET-28a/*osc-lox*-A296G were cultivated in 1 L of LB medium containing 50 μg mL^{-1} kanamycin at 37 °C. Expression of Osc-LOX-A296G was induced by adding 0.01 mM isopropyl-β-thiogalactopyranoside when reaching an optical density of 0.6 (600 nm), and incubating at 20 °C for 24 h on shaking incubator at 180 rpm.

2.2. Enzyme purification and measurement of molecular weight

After expression, cultured cells containing Osc-LOX-A296G were harvested by centrifugation at 3500 × g for 15 min at 4 °C. Cell pellet was resuspended in 50 mL lysis buffer (50 mM Tris-HCl pH 7.5, 500 mM NaCl, 10 mM imidazole, 0.1 mM PMSF, and 5% glycerol). The resuspended cells were lysed by a sonicator. Cell debris was eliminated by centrifugation at 13,000 × g for 30 min at 4 °C and the supernatant was filtered by a syringe filter (0.45 μm). The soluble fraction was loaded onto a cobalt affinity column (HiTrap Talon crude 5 mL, GE Healthcare, WI, USA) equilibrated with lysis buffer. Cobalt column was washed by 5 CV wash buffer (50 mM imidazole added to lysis buffer) to remove nonspecific binding proteins. The crude proteins were fractionated by increasing concentrations of imidazole up to 700 mM at flow rate of 5 mL min^{-1}. Fractions harboring target protein were concentrated by Amicon Ultra-15 (10 kDa cut-off). Concentrated proteins were loaded onto a size-exclusion chromatography (SEC) column (HiLoad 16/600 Superdex 200 prep grade, GE Healthcare, WI, USA) that had been previously equilibrated with SEC buffer (50 mM Tris-HCl pH 7.5, 150 mM NaCl) and was separated at a flow rate of 1 mL min^{-1}. Also, SEC was utilized to confirm the molecular weight and oligomeric state. The SEC standards, thyroglobulin (670 kDa), γ-globulin (158 kDa), ovalbumin (44 kDa), myoglobulin (17 kDa), and vitamin B12 (1.35 kDa), were used for calibration. The molecular weight was calculated by comparison with the elution time of standards.

2.3. Effects of pH and temperature in enzyme reactions

Purified Osc-LOX-A296G was used to confirm the optimum catalytic conditions of pH and temperature toward linoleic acid (LA; C18:2 n-$6^{\Delta 9,12}$, TCI chemicals, Tokyo, Japan). All reactions for assay were carried out using 3 μg mL^{-1} enzyme and 50 μM LA for 10 min. The optimum pH was monitored over a range of pH values from 5.0 to 10.0 at room temperature. The buffers were 2-(*N*-morpholino) ethanesulfonic acid (MES) buffer (50 mM, pH 5.0), sodium phosphate buffer (50 mM, pH 6.0 and 7.0), Tris-HCl buffer (50 mM, pH 8.0), and sodium tetraborate buffer (50 mM, pH 9.0 and 10.0). To investigate optimum temperature, the reaction mixtures (enzyme with 50 mM Tris-HCl buffer, pH 8.0) without substrate were pre-heated for 30 min at different temperatures ranging from 20 to 60 °C. And then, the activity was measured by adding substrates for 10 min.

2.4. Specific activity and kinetics toward PUFAs

The specific activity and kinetic parameters of Osc-LOX-A296G toward arachidonic acid (AA; 20:4 n-$6^{\Delta 5,8,11,14}$, TCI chemicals, Tokyo, Japan), eicosapentaenoic acid (EPA; 20:5 n-$3^{\Delta 5,8,11,14,17}$, TCI chemicals, Tokyo, Japan), and docosahexaenoic acid (DHA; 22:6 n-$3^{\Delta 4,7,10,13,16,19}$, Glentham Life Science, Corsham, UK) were determined by monitoring the increase in the formation rate of the conjugated diene (monohydroperoxide) at absorbance at 234 nm. The enzymatic reaction was carried out using 50 mM Tris-HCl buffer (pH 8.0), 3 μg mL^{-1} enzyme and varying amounts of the substrate from 25 to 125 μM at 30 °C for 5 min in a quartz cuvette (10 mm), and all reactions were repeated three times. The absorbance was recorded every 2 s by an Ultrospec 3100 Pro spectrophotometer (Amersham Biosciences, Cambridge, UK). The extinction coefficient, $\varepsilon = 2.3 \times 10^4\ M^{-1}\ cm^{-1}$ for the formation of conjugated diene was used to calculate enzymatic activity [7]. One Unit of the enzyme was defined by the amount required for the transformation of 1 μmol into hydroperoxy fatty acids (HpFAs) per minute. For kinetic parameters, reaction rates were calculated from the initial linear portion of the curve. The Michaelis constant (K_m) and turnover number (k_{cat}) were calculated by nonlinear-regression fits to the Michaelis-Menten equation using the SigmaPlot 10.0 software.

2.5. Enzyme reactions for conversion of LA and DHA into hydroxy fatty acids (HFAs)

Enzymatic reactions were performed to convert LA and DHA into HFAs. The reaction mixture was prepared so as to contain 50 μM substrate in 50 mM Tris-HCl buffer (pH 8.0). For DHA conversion, enzyme reaction was initiated by adding Osc-LOX-A296G of 50, 100, and 200 Units per mL of reaction volume, respectively, while 100 Units were used for LA conversion. The reaction mixture was incubated at 30 °C with magnetic stirring for 30 min. Hydroperoxide products were reduced by the addition of sodium borohydride to a final concentration of 25 mM for 10 min, after which enzyme reactions were finished by adding glacial acetic acid (5 μL mL^{-1}). The converted products were refined using HP20 (Mitsubishi Chemical, Tokyo, Japan) resin one-twentieth of the reaction volume. The HFAs were identified by HPLC and LC-MS/MS analysis.

2.6. HPLC analysis

Agilent 1200 series (Agilent Technologies, Waldbronn, Germany) was utilized for analysis of Osc-LOX-A296G reaction products. Chiral-phase HPLC (CP-HPLC) was performed isocratically on a

CHIRALCEL OD-H column (25 cm × 4.6 mm, 5 μm particle size, DAICEL, Tokyo, Japan) using the solvent consisting of *n*-hexane/2-propanol/acetic acid (95:5:0.1, by volume). The flow rate was 1.0 mL min^{-1}, and the column temperature was maintained at 30 °C. Normal-phase HPLC (NP-HPLC) was equipped with a SUPELCOSIL LC-DIOL column (25 cm × 3 mm, 5 μm particle size, SUPELCO, Sigma-Aldrich). A mobile phase consisting of heptane/2-propanol/acetic acid (95:5:0.1, by volume) was used at a flow rate of 0.5 mL min^{-1} and a column temperature of 10 °C for NP-HPLC analysis. All samples were prepared in mobile phase and were injected 10 μL. The reaction products were detected by monitoring absorbance at 237, 242, and 270 nm, and identified by comparing retention times using HFA standards, 9*S*-, 9*R*-, 13*S*-, 13*R*-hydroxyoctadecadienoic acid (HODE), and (±)13-hydroxy docosahexaenoic acid (13-HDHA) (Cayman Chemical, MI, USA). The amounts of conversion products were measured by correlating peak areas with concentrations of reference material in linear calibration curves. Converted products were purified by a SUPELCOSIL LC-DIOL column with a fraction collector and they were used for NMR analysis.

2.7. LC-MS/MS analysis

LC-MS/MS analysis of HFAs converted from DHA was performed by an Agilent TOF spectrometer G6550A (Agilent Technologies, Santa Clara, CA, U.S.) equipped with an electrospray ionization (ESI) interface. The conversion products were separated on a ZORBAX Eclipse Plus C18 column (10 cm × 2.1 mm, 1.8 μm particle size, Agilent) with a isocratic solvent of water/acetonitrile/formic acid (90:10:0.1, by volume) at a column temperature of 40 °C and a flow rate 0.3 mL min^{-1}. All analyzed samples were prepared in absolute ethanol and were injected 2 μL. Sample ionization was performed in negative mode using the following conditions: nitrogen (14 L min^{-1}, 200 °C) drying gas; 35 psi nebulizer gas; 3.5 kV capillary voltage; 350 °C capillary temperature; and 20V fragmentor voltage in negative mode. Spectra were recorded over an *m/z* range of 0–500 with an accumulation rate of 2 spectra/s. Data were processed using Mass Hunter Workstation Acquisition software and the molecular masses of its fragments were confirmed by ChemDraw Professional v 15.1.

2.8. Nuclear magnetic resonance (NMR) spectroscopy

NMR analysis was performed on Bruker Avance III HD spectrometer (800-MHz) equipped with a 5 mm triple resonance inverse (TCI) Cryo Probe. 5–10 mg HFAs were dissolved in 700 μL methanol-D4 and measured at 298 K. Besides 1D ^{1}H and ^{13}C NMR, the following 2D-NMR were performed: $^{1}H-^{1}H$ COSY, $^{1}H-^{1}H$ TOCSY, $^{1}H-^{13}C$ HSQC, and $^{1}H-^{13}C$ HMBC. NMR data were assigned using NMRViewJ software.

3. Results and discussion

Site-directed mutagenesis was performed to investigate whether substitution of amino acid could control catalytic properties. The amino acid sequence-alignment analysis was carried out with conserved sequences of previously identified LOXs of animals, plants, and bacteria. Alanine (*S*-type) and glycine (*R*-type) in the catalytic pocket of LOXs are conserved as stereo- and regiospecificity determinant known as the Coffa-Brash sequence [5] (Fig. 1). Wild-type Osc-LOX contains alanine at amino acid 296 and it has been identified as linoleate 13*S*-LOX in our previous study. The gene (1713 bp) encoding mutant Osc-LOX that alanine 296 was replaced by glycine was cloned into pET-28a. Osc-LOX-A296G was expressed by *E. coli* system. Molecular weight of A296G including a His-tag was theoretically estimated of 67.2 KDa (Fig. 2A, left). Osc-LOX-

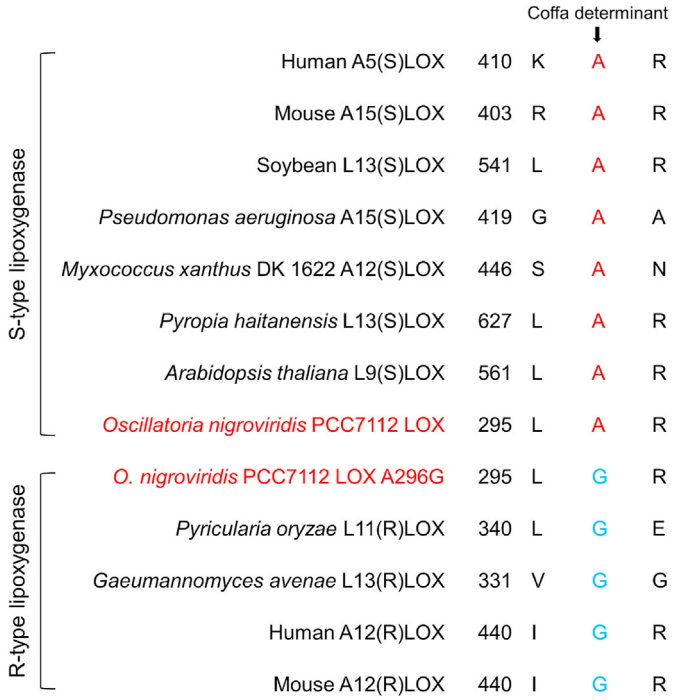

Fig. 1. Amino acid sequence alignment of various *S*- and *R*-LOXs with Osc-LOX-A296G. The highlighted amino acid indicate that Ala is conserved in *S*-type LOX and Gly is conserved in *R*-type LOX.

A296G was purified by following two-step chromatography: first, Osc-LOX-A296G was isolated over an imidazole concentration range of 170–190 mM by cobalt affinity column. (Fig. 2A, middle). Next, SEC was performed for obtaining further purified protein and for measurement of protein molecular weight. Osc-LOX-A296G was eluted at 82 min. The molecular weight was confirmed as approximately 67.55 kDa compared to the retention times of the standars, indicating that it exists as a monomer (Fig. 2A, right and 2B). We have obtained 12.5 mg of the purified functional enzyme with purity of 93% from a 1-L culture, which was 2.5-fold higher than soybean LOX obtained by *E. coli* BL21 (DE3) [8]. Moreover, murine 12*R*-LOX was expressed in *E. coli* system at low yield that could not be used in enzyme reaction [9]. This result suggests that bacterial LOXs could be efficiently expressed with higher yield more than eukaryotic LOXs.

The effects of pH and temperature on the enzyme activity were investigated by monitoring the conversion yield of HpFA from LA using the spectroscopic method with 234 nm UV. The maximum activity on the various pH and temperatures was defined as 100%, and the relative activity was plotted as a percentage. Osc-LOX-A296G showed maximum activity at pH 8.0 (Fig. 2C). Some plant-derived acidic LOXs have been found, but most LOXs prefer neutral or alkaline pH conditions [10,11]. The optimum temperature was confirmed to be 30 °C (Fig. 2D), and the enzyme was stable from 20 to 35 °C without aggregation. However, its activity rapidly declined above 40 °C and was totally lost at temperatures above 55 °C with aggregation. Although a slight quantitative change compared to the wild-type, these results showed the altered amino acids did not affect the optimum activity by pH and temperature.

The specific activity (μmol min^{-1} mg^{-1}) and catalytic efficiency (min^{-1} μM^{-1}) toward AA, EPA, and DHA were calculated as follows: 4768.9 and 9.7; 3148.9 and 6.2; 3084.1 and 6.0, respectively (Table S1). The Michaelis-Menten plots of each substrates are provided in Fig. S1. These results showed that enzymatic activity was significantly decreased compared with wild-type. In particular, the

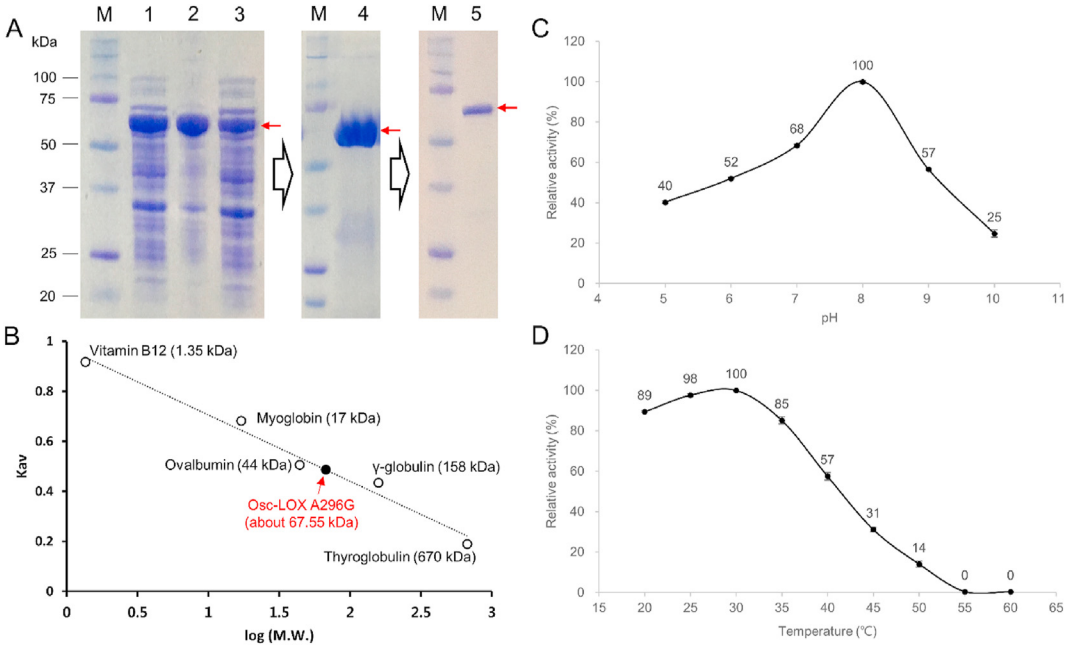

Fig. 2. Purification and enzymatic characterization of Osc-LOX-A296G. (A) Left, expression and solubility were confirmed by SDS-PAGE. The molecular weight of Osc-LOX-A296G (67.2 kDa) containing a His-tag was confirmed by comparison with protein marker (lane-1, after induction; lane-2, insoluble friction; lane-3, soluble fraction). Middle, purified enzyme by cobalt affinity chromatography. Right, highly purified enzyme by size-exclusion chromatography (SEC). (B) The molecular weight and oligomeric state of purified enzyme were determined using SEC on a HiLoad 16/600 Superdex 200 pg. Target protein was eluted at a position corresponding to 67.5 kDa (filled circle) as a monomer in aqueous solution. Effect of pH (C) and temperature (D) on the enzymatic activity.

specific activity and catalytic efficiency of the variant toward AA were reduced by 37.1% and 43.3%, respectively. It has been previously reported that site-directed mutagenesis, which switches Ala to Gly, bring about reducing enzymatic activity with changing regio- and stereochemistry [9].

To confirm the catalytic effect of substituted amino acid on the regio- and stereospecificity, we performed enzymatic reactions with LA. HpFA was generated and its hydroperoxide group was converted into alcohol groups by sodium borohydride. The HFA deoxygenated was identified by comparing the retention times with those of standards using CP-HPLC. The 13*S*-HODE formed by wild-type was used as a reference to confirm the changed properties by A296G. The retention times of four standards, 9*S*-, 9*R*-, 13*S*-, and 13*R*-HODE, were 12.2, 11.28, 10.8, and 8.7 min, respectively. The HFA produced by Osc-LOX-A296G was eluted at accurately the same time as the 9*R*-HODE standard (Fig. 3A). The concentration of 9*R*-HODE converted from 50 μM LA was 45.8 μM (conversion rate 91.6%). Osc-LOX-A296G completely converted LA into 9*R*-HODE, not 13*S*-HODE. Thus, these results indicate that the property of wild-type as linoleate 13*S*-LOX was totally changed to linoleate 9*R*-LOX by substitution Ala to Gly. According to reported studies, the changes of regio- and stereospecificity, such as that the 13(*S* or *R*)-HODE to the 9(*R* or *S*)-HODE or vice versa, by the Ala and Gly exchange were related to the size of amino acid adjacent to the carbon where oxygen could be inserted [5].

Two products were generated from DHA depending on the concentration of enzyme ranging from 50 to 200 Unit mL^{-1} (Fig. 3B). In NP-HPLC, the first product generated at concentration of 50 Unit mL^{-1} was eluted at 5.78 min (λ_{max} of 237 nm), which matched the retention time of the (±)13-HDHA standard. DHA appears to be totally consumed by enzyme reaction using 50 Unit mL^{-1} because the peak of remaining substrate was no detected (data not shown), however, this result does not mean that DHA was converted into first product as 100%. The concentration of the first product converted from 50 μM DHA was 41 μM (conversion rate 82%). The final product formed by concentrations of 100–200 Unit mL^{-1} was detected at 16.3 min at a λ_{max} of 270 nm. The conversion of the final product from 13-HDHA was initiated at a concentration of 100 Unit mL^{-1}, but the full conversion was completed using a concentration of 200 Unit mL^{-1}, which was yielded 30 μM corresponding to a conversion rate of 73% from the first product. The concentration of two products was determined by reference to a calibration curve generated using purified products by preparative HPLC. We have estimated that the final product has a molecular structure of 13,20-dihydroxy- docosahexaenoic acid. Our assumption could be supported by the following two pieces of evidence. First, the peak corresponding to 13-HDHA decreased and the latter peak was newly generated by the increasing concentration of the enzyme, thus the final product was generated from the first product. LOX is known to be an irreversible enzyme, so higher concentrations of the enzyme are required to catalyze dihydroperoxy fatty acid [12]. Finally, the final product was detected at a λ_{max} of 270 nm UV with a triplet spectrum (260, 270, and 280 nm); this spectrum represents that it has a conjugated triene. The second hydroxyl group must be introduced into carbon-20 to form a conjugated triene, because HFAs have unique spectra reflecting their conjugated double bonds [13]. Two products were further analyzed by CP-HPLC comparing with standards, 13*S*- and 13*R*-HDHA, to verify the regio- and stereochemistry. The retention times of the first and final products were 11 and 52.8 min, respectively (Fig. 3C). These results indicated that the first product is 13*R*-HDHA however the final product did not match any standards.

To identify total molecular mass of two products, we carried out LC-MS analysis in negative ion mode [M-H$^-$]. First product confirmed as 13*R*-HDHA was detected at *m*/*z* 343.2 [M-H-] corresponding to molecular mass of a monohydroxy-DHA (344.24 Da; $C_{22}H_{32}O_3$), and the final product was detected at *m*/*z* 359.2 [M-H$^-$] corresponding to a dihydroxy-DHA (360.23 Da; $C_{22}H_{32}O_4$) (Fig. S2). Also, the final product was further analyzed by LC-MS/MS (Fig. 4). Two fragment peaks at *m*/*z* 167 and 193 were formed by cleavage

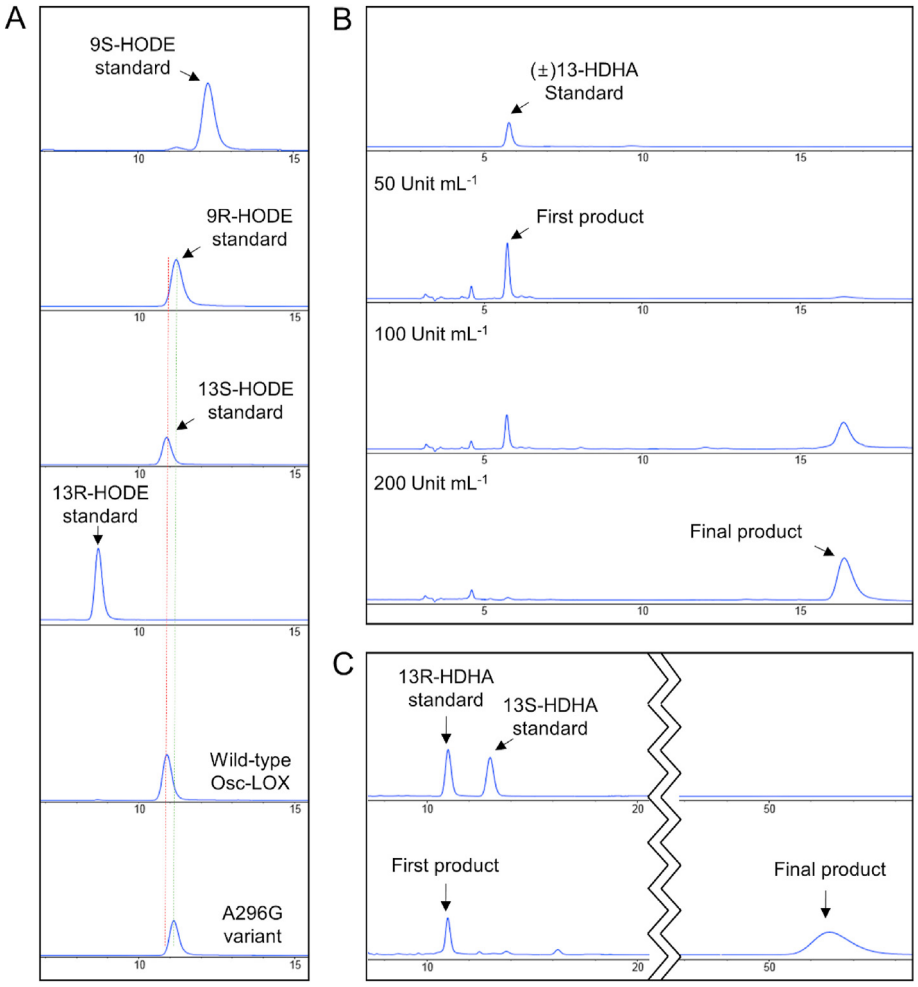

Fig. 3. HPLC analysis of HFAs generated from LA and DHA by Osc-LOX-A296G. (A) CP-HPLC analysis for regio- and stereospecificity determination for linoleic acid. The product generated by Osc-LOX A296G was identified 9R-HODE. (B) NP-HPLC profile of two products obtained from DHA. First product (13-HDHA) was generated by enzyme concentration of 50 Unit mL^{-1}. Final product was converted from 13-HDHA by enzyme concentration of 200 Unit mL^{-1}. (C) CP-HPLC profile to confirm the stereochemistry of the first product (13*R*-HDHA).

between C-12 and C-13, respectively. These peaks indicate that two hydroxyl groups may exist between C-13 and C-22. Another fragment peak formed by cleavage between C-13 and C-14 was detected at *m*/*z* 137. This fragment including a methyl group contains one hydroxyl group, and also means that another hydroxyl group was formed at the C-13. A small fragment generated by cleavage between C-19 and C-20 was detected at *m*/*z* 59, consequently indicating that it was hydroxylated at carbon-20. Thus, the final product has two hydroxyl groups at C-13 and C-20.

The structural configurations of two products were accurately determined by 800-MHz NMR spectroscopy. The spectra of 1D-NMR and 2D-NMR for the first product identified as 13*R*-HDHA were shown in Fig. S3 and Fig. S4, respectively, and assigned chemical shifts were summarized in Table S2. The chemical shifts of the C13—OH was recorded at 4.13 ppm (^{1}H) and 73.94 ppm (^{13}C) in 2D ^{1}H—^{13}C HSQC spectrum (Fig. S7A). The ^{1}H NMR spectrum showed that a conjugated diene fragment as 14*E*,16*Z* was determined to be the *trans*-geometry between C-14 and C-15 based on the coupling constants of J14 and J15 (15.92 Hz). *Cis* (*Z*) and *trans* (*E*) coupling appear differently on ^{1}H NMR spectrum [14]. The coupling constant of the olefinic protons shows approximately ranging of 12—19 Hz in *trans*-geometry and 7—11 in *cis*-geometry. Thus, these results indicated that the chemical structure of the first product was as 13*R*-hydroxy-4*Z*,7*Z*,10*Z*,14*E*,16*Z*,19*Z*-docosahexaenoic acid. The NMR spectra of final product were shown in Fig. S5 and Fig. S6, and assigned chemical shifts were summarized in Table S2A. The chemical shifts corresponding to C13—OH and C20—OH were detected as follows: C13—OH, 4.17 ppm (^{1}H) and 73.81 ppm (^{13}C); C20—OH, 4.04 ppm (^{1}H) and 75.40 ppm (^{13}C) in 2D ^{1}H—^{13}C HSQC spectrum (Fig. S7B). The ^{1}H NMR spectrum exhibited that the geometry of conjugated triene fragment was 14*E*,16*Z*,18*E* based on the coupling constants of J14-J15 (15.92 Hz) and J18-J19 (12.72 Hz). Based on these results, the chemical structure of the final product was determined to be 13*R*,20-dihydroxy-4*Z*,7*Z*,10*Z*,14*E*,16*Z*,18*E*-docosahexaenoic acid (13*R*,20-diHDHA). However, we have could not define the stereochemistry of C20—OH due to insufficient data, thus it would be required additional NMR experiments such as NOESY or ROESY.

In conclusion, we obtained two HFAs identified as a 13*R*-HDHA and a 13*R*,20-diHDHA from DHA by Osc-LOX-A296G. It was reported that the 13-HDHA inhibited IL-1β, which is a potent pro-inflammatory cytokine, generating by microglial cells, and the 13,20-diHDHA converted from 13-HDHA was discovered in the resolution phase of inflammation [15]. It was reported that the 13-HDHA was synthesized by recombinant human cyclooxygenase-2 expressed in Sf9 insect cells. The 13,20-diHDHA was discovered as a metabolite converted from 13-HDHA by unknown enzymatic reaction *in vivo* [15]. To the best of our knowledge, this is the first

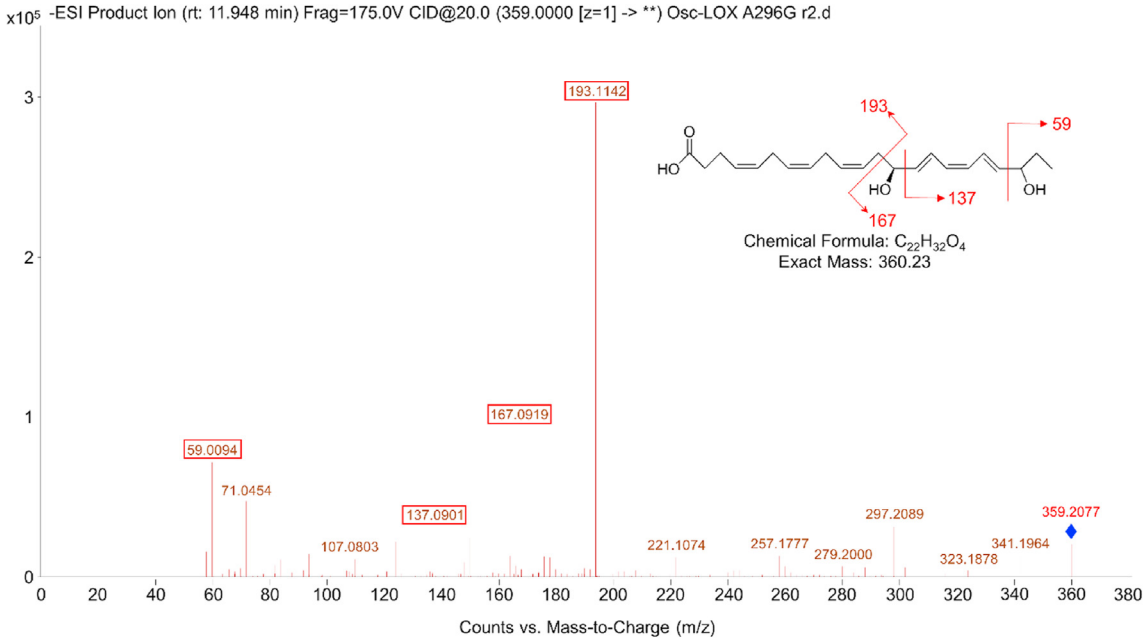

Fig. 4. LC-MS/MS analysis of 13*R*,20-dihydroxy-docosahexaenoic acid (13R,20-diHDHA). This fianl product was generated from DHA via 13*R*-HDHA by Osc-LOX-A296G. The blue rhombus square indicates total molecular mass of 13*R*,20-diHDHA and the empty red squares indicate molecular masses of fragments.

report of efficient production of human endogenous 13*R*-HDHA and 13*R*,20-diHDHA through *in vitro* enzymatic reactions. Thus, our finding may enable physiological studies and pharmaceutical research for the 13*R*,20-diHDHA.

Note: While submitting this manuscript, a paper describing wild-type LOX was first submitted and is under revision for publishing.

Declaration of competing interest

The authors declare that they have no known competing financial interests or personal relationships that could have appeared to influence the work reported in this paper.

Acknowledgments

This work was supported by grants from the Korea Research Foundation (KRF) for Basic Research Promotion (2017R1A2B4006016) and from the KRIBB Research Initiative Program (KGM5482012). This study also partly supported by the GRRC program of Gyeonggi province (GRRC-CHA2017-A01, Discovery and Analysis of Regional Specialized Resources and Operation of Regional Research Service Center).

Appendix A. Supplementary data

Supplementary data to this article can be found online at https://doi.org/10.1016/j.bbrc.2020.09.079.

References

[1] I. Ivanov, D. Heydeck, K. Hofheinz, J. Roffeis, V.B. O'Donnell, H. Kuhn, M. Walther, Molecular enzymology of lipoxygenases, Arch. Biochem. Biophys. 503 (2010) 161–174.
[2] J. Groot, G.A. Veldink, J. Vliegenthart, J. Boldingh, R. Wever, B. Van Gelder, Demonstration by EPR spectroscopy of the functional role of iron in soybean lipoxygenase-1, Biochim. Biophys. Acta 377 (1975) 71–79.
[3] S.T. Prigge, B.J. Gaffney, L.M. Amzel, Relation between positional specificity and chirality in mammalian lipoxygenases, Nat. Struct. Biol. 5 (1998) 178–179.
[4] S.A. Gillmor, A. Villaseñor, R. Fletterick, E. Sigal, M.F. Browner, The structure of mammalian 15-lipoxygenase reveals similarity to the lipases and the determinants of substrate specificity, Nat. Struct. Biol. 4 (1997) 1003–1009.
[5] G. Coffa, A.R. Brash, A single active site residue directs oxygenation stereospecificity in lipoxygenases: stereocontrol is linked to the position of oxygenation, Proc. Natl. Acad. Sci. Unit. States Am. 101 (2004) 15579–15584.
[7] C. Cossette, P. Patel, J.R. Anumolu, S. Sivendran, G.J. Lee, S. Gravel, F.D. Graham, A. Lesimple, O.A. Mamer, J. Rokach, Human neutrophils convert the sebum-derived polyunsaturated fatty acid sebaleic acid to a potent granulocyte chemoattractant, J. Biol. Chem. 283 (2008) 11234–11243.
[8] D. Tomchick, P. Phan, M. Cymborowski, W. Minor, T. Holman, Structural and functional characterization of second-coordination sphere mutants of soybean lipoxygenase-1 †, Biochemistry 40 (2001) 7509–7517.
[9] S. Meruvu, M. Walther, I. Ivanov, S. Hammarström, G. Fürstenberger, P. Krieg, R. Pallu, H. Kühn, Sequence determinants for the reaction specificity of murine (12R)-lipoxygenase - targeted substrate modification and site-directed mutagenesis, J. Biol. Chem. 280 (2005) 36633–36641.
[10] S. Hayward, T. Cilliers, P. Swart, Lipoxygenases: from isolation to application, Compr. Rev. Food Sci. Food Saf. 16 (2017) 199–211.
[11] S. Liu, B. Han, Differential expression pattern of an acidic 9/13-lipoxygenase in flower opening and senescence and in leaf response to phloem feeders in the tea plant, BMC Plant Biol. 10 (2010) 228.
[12] O. Rådmark, O. Werz, D. Steinhilber, B. Samuelsson, 5-Lipoxygenase: regulation of expression and enzyme activity, Trends Biochem. Sci. 32 (2007) 332–341.
[13] C. Serhan, J. Dalli, R. Colas, J. Winkler, N. Chiang, Protectins and maresins: new pro-resolving families of mediators in acute inflammation and resolution bioactive metabolome, Biochim. Biophys. Acta 1851 (2014).
[14] E. Alexandri, R. Ahmed, H. Siddiqui, M. Choudhary, C. Tsiafoulis, I. Gerothanassis, High resolution NMR spectroscopy as a structural and analytical tool for unsaturated lipids in solution, Molecules 22 (2017) 1663.
[15] C.N. Serhan, S. Hong, K. Gronert, S.P. Colgan, P.R. Devchand, G. Mirick, R.L. Moussignac, Resolvins, A family of bioactive products of omega-3 fatty acid transformation circuits initiated by aspirin treatment that counter proinflammation signals, J. Exp. Med. 196 (2002) 1025–1037.